sustainable chemistry

MDPI

Article

Valorization of Thermoplastic Polyurethane and Styrofoam Waste for Development of Improved Sustainable Blend Membranes

Tutik Sriani [1], Tatiya Wannomai [2,†], Thanongsak Thepsonthi [3], Chandrawati Putri Wulandari [4,5], Rizky Astari Rahmania [4,5], Muslim Mahardika [6], Norihisa Miki [7] and Gunawan Setia Prihandana [4,5,*]

[1] Department of Research and Development, PT. Global Meditek Utama-IITOYA, Sardonoharjo, Ngaglik, Sleman, Yogyakarta 55581, Indonesia; tsriani@iitoya.com
[2] Department of Chemical Engineering, Faculty of Engineering, Burapha University, 169 Longhard Bangsaen Beach Rd., Saensook, Muang, Chonburi 20131, Thailand
[3] Department of Industrial Engineering, Burapha University, 169 Longhard Bangsaen Beach Rd., Saensook, Muang, Chonburi 20131, Thailand; thanongsak@eng.buu.ac.th
[4] Department of Industrial Engineering, Faculty of Advanced Technology and Multidiscipline, Universitas Airlangga, Jl. Dr. Ir. H. Soekarno, Surabaya 60115, Indonesia; chandrawati.p.w@ftmm.unair.ac.id (C.P.W.); rizky.astari@ftmm.unair.ac.id (R.A.R.)
[5] Research Group of Industrial Management, System Engineering & Manufacturing, Universitas Airlangga, Jl. Dr. Ir. H. Soekarno, Surabaya 60115, Indonesia
[6] Department of Mechanical and Industrial Engineering, Faculty of Engineering, Universitas Gadjah Mada, Jalan Grafika No. 2, Yogyakarta 55281, Indonesia; muslim_mahardika@ugm.ac.id
[7] Department of Mechanical Engineering, Keio University, 3-14-1 Hiyoshi, Kohoku-ku, Yokohama 223-8522, Japan; miki@mech.keio.ac.jp
* Correspondence: gunawan.prihandana@ftmm.unair.ac.id; Tel.: +62-881-0360-00830
† Deceased author.

Abstract

This study aimed to improve the mechanical integrity of Styrofoam membranes fabricated from post-consumer food packaging. To this end, 3D-printing byproduct—thermoplastic polyurethane (TPU) waste—was blended with polyimide (PI) in the membrane dope solution. The synthesized flat-sheet upcycled membranes were evaluated via scanning electron microscopy (SEM), water contact angle (WCA), and tensile testing, while separation efficiency was determined through bovine serum albumin (BSA) rejection and permeation trials. Findings indicate that incorporating TPU into the Styrofoam/PI matrix increased tensile strength by 50%, BSA rejection by 12.4%, and permeation by 33%. Compared with pristine Styrofoam membranes, tensile strength and BSA rejection improved by 240% and 46%, respectively. Although the blend membranes exhibited a reduction in water flux (from 214 to 162.5 LMH/bar) due to pore contraction, they maintained high rejection rates (~86%) for large macromolecules like PVP (1300 kDa). Furthermore, while all membranes remained hydrophilic, hydrophobicity scaled with TPU concentration.

Keywords: Styrofoam; upcycle; membrane; TPU; plastic waste; clean water

Check for updates

Academic Editors: Carol López-de-Dicastillo, Eliezer Velásquez and Adrián Rojas Sepúlveda

Received: 11 May 2026
Revised: 7 June 2026
Accepted: 15 June 2026
Published: 19 June 2026

Copyright: © 2026 by the authors. Licensee MDPI, Basel, Switzerland. This article is an open access article distributed under the terms and conditions of the Creative Commons Attribution (CC BY) license.

1. Introduction

While the modern era relies heavily on the versatility and durability of plastics, the resulting environmental toll—particularly from single-use variants—has reached a critical threshold. Current projections suggest global plastic consumption will nearly double from 464 million tons in 2020 to 884 million tons by 2050 [1]. Despite packaging accounting for 40% of production, recycling rates remain dismal; over 60% of plastic

packaging has gone unrecycled over the last sixty years, often being downcycled into low-value materials that preclude further recovery [2,3]. Even in advanced economies, waste volumes frequently outpace processing infrastructure [4]. Expanded polystyrene (EPS), or Styrofoam, exemplifies this crisis. Although valued for its thermal insulation and lightweight properties in food packaging, its 98% air composition renders transport to recycling centers economically unviable [5]. As polystyrene production continues to scale, there is an imperative to transition from traditional disposal toward high-value upcycling strategies that convert EPS waste into functional materials.

Forecasts suggesting that the European Union may reach full plastic circularity by 2050 point to a future shift away from waste-to-energy models [1]. However, the regulation of primary production [6] does not adequately address the persistent issue of secondary microplastics [7]. The environmental hazard is particularly pronounced for Styrofoam; its microplastic derivatives exhibit size-dependent toxicity exacerbated by UV exposure [8]. Consequently, the transformation of post-consumer waste into high-performance materials serves as a robust environmental safeguard [9]. Upcycling thus serves a dual purpose: it prevents the formation of toxic micro-fragments while reclaiming the economic and functional value of the polymer matrix.

Over the last decade, polystyrene (PS) has constituted approximately 10% of global plastic waste by weight [5]. It remains one of the most recalcitrant post-consumer polymers, with recycling rates lagging significantly behind other plastics [10]. Currently, Styrofoam recycling is dominated by thermal and catalytic decomposition into oil-like derivatives [11]. While some researchers have explored high-yield (80%) upcycling strategies to synthesize acylated (PSA) and brominated (PSB) polystyrene [12], others have investigated hybrid thermal-biodegradation pathways using *Pseudomonas putida* and *Salmonella* to produce benzene and naphthalene [13]. Despite their potential to reduce the 30% contribution of PS to landfill volume, these biological processes are often too time-intensive for industrial scaling. Alternatively, circular economy models suggest blending 30% post-consumer Styrofoam with virgin and scrap resins to maintain material quality [14]. However, chemical modification to transform Styrofoam into value-added products offers superior potential for functional enhancement compared with simple mechanical recycling [15]. Recent advances have successfully repurposed Styrofoam waste into specialized adsorbents for wastewater treatment [16], heavy metal remediation [17,18], and oil or chemical sorption [19,20].

This study sought to bolster the mechanical strength of upcycled Styrofoam waste membranes, extending the research initiated by Sriani et al. [21] through the strategic incorporation of 3D-printing-derived TPU waste. TPU is established in the literature as an effective additive for enhancing the toughness, wear resistance, and thermal stability of polymer blends [22–24]. Here, the influence of TPU concentration on membrane structure was examined via SEM (Phenom ProX, Thermo Fisher Scientific Inc., Waltham, MA, USA), and its impact on functional performance was quantified using tensile testing, hydrophobicity measurements (WCA), and separation trials involving pure water flux and protein rejection.

2. Materials and Methods

2.1. Synthesis of Styrofoam Waste Solution

The preparation of the Styrofoam dope solution followed the protocol described in our previous work [21]. Briefly, cleaned and vacuum-dried Styrofoam containers were shredded into small fragments. To prepare the base solutions, the shredded Styrofoam was dissolved in N-Methyl-2-Pyrrolidone (NMP) (Merck KGaA, Darmstadt, Germany) in six separate glass flasks to achieve a 20 wt.% concentration, with heating at 80 °C to ensure complete dissolution. One flask was reserved as the native Styrofoam control.

To the remaining five flasks, 6 wt.% polyimide (PI) was introduced and reheated until a homogeneous mixture was achieved. PI was strategically chosen as the primary additive based on prior research [21], which highlighted its ability to improve the separation performance of upcycled Styrofoam matrices. Specifically, PI transforms narrow macrovoids into rounded structures, stabilizing water flux and significantly enhancing solute rejection. Therefore, this optimized 6 wt.% Styrofoam/PI blend served as the high-rejection base matrix. To mitigate the membrane's inherent mechanical fragility, recycled thermoplastic polyurethane (TPU)—derived from 3D printing byproducts processed at 140 °C, cooled, and pelletized—was added to the solutions at concentrations of 0, 0.25, 0.5, 0.75, and 1.0 wt.%. The mixtures were heated and continuously stirred for three hours to ensure uniform dispersion of all additives. Finally, the homogeneous dope solutions were left to naturally degas and cool to room temperature. Table 1 details the final membrane compositions. Analytical-grade PI and NMP were supplied by Merck KGaA, Darmstadt, Germany).

Table 1. Compositions of the Styrofoam waste blend membranes.

Membrane	Styrofoam (wt.%)	PI (wt.%)	TPU (wt.%)	NMP (wt.%)
#M0	20	0	0	80
#M1	20	6	0	74
#M2	20	6	0.25	73.75
#M3	20	6	0.5	73.5
#M4	20	6	0.75	73.25
#M5	20	6	1.0	73

2.2. Fabrication of Styrofoam Blend Membrane

The membranes were fabricated using the non-solvent-induced phase separation (NIPS) method. The cooled dope solution was cast onto a clean glass plate at a controlled wet thickness of 100 µm using a manual casting blade (Elcometer, Manchester, UK). Immediately following casting, the glass plate was immersed in a coagulation bath containing deionized water to induce phase inversion. The resulting membranes were subsequently stored in pure water for 24 h to ensure the complete removal of residual solvents before further characterization. The schematic representation of the membrane preparation and fabrication workflow is illustrated in Figure 1.

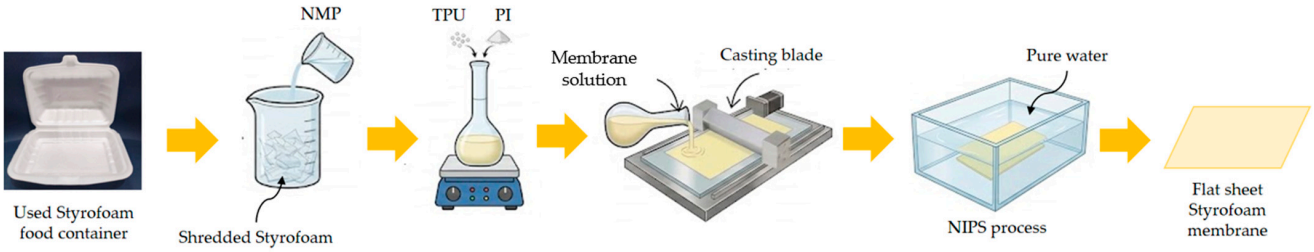


Figure 1. The fabrication process of Styrofoam waste membrane.

2.3. Permeation and Separation Test

Membrane permeation and separation performance were evaluated using a dead-end filtration system (HP4750 Stirred Cell, Sterlitech Corp., Kent, WA, USA), consistent with the experimental setup described in our previous study [21]. The effective filtration area of the membrane was 14.6 cm^2. To ensure a stable flux, each membrane was pre-compacted and tested for 30 min before data collection. Filtration was driven by nitrogen gas at a constant operating pressure of 1 bar. The mass of the permeate was continuously monitored

and recorded using a Weighing Environment Logger (AD-1687, A&D, Tokyo, Japan). The permeation flux (J_v) was subsequently calculated using the following equations:

$$J_v = \frac{Q}{A \times \Delta t} \quad (1)$$

$$L_p = \frac{J_v}{\Delta P} \quad (2)$$

The volumetric flux (J_v) and permeability (L_p) were calculated according to the following definitions: Q represents the permeate volume (L) collected during the sampling interval Δt, A is the effective membrane area (m^2), ΔP is the transmembrane pressure (bar).

Protein separation performance was evaluated using a dead-end filtration cell at a constant pressure of 1 bar. A 0.1 wt.% solution of Bovine Serum Albumin (BSA, MW 65 kDa; Himedia Laboratories Pvt. Ltd., Mumbai, India) was prepared in phosphate-buffered saline (PBS) at pH 7.2. The resulting permeate was collected and the BSA concentration was quantified using an N4S UV-Visible Spectrophotometer (Ningbo Hinotek Instrument Co., Ltd., China) at a wavelength of 280 nm. The solute rejection (SR) was determined using the following expression:

$$\%SR = \left[1 - \frac{C_p}{C_f}\right] \times 100 \quad (3)$$

where C_p and C_f represent the BSA concentrations in the permeate and feed solutions (wt.%), respectively. To further evaluate the separation capacity for larger macromolecules, an additional rejection test was conducted using a 0.1 wt.% solution of polyvinylpyrrolidone (PVP, MW 1300 kDa; Merck & Co., Inc., Rahway, NJ, USA) in deionized water. As the molecular weight of PVP is approximately 20 times greater than that of BSA, it served as a representative high-molecular-weight solute to assess the size-exclusion limits of the membranes.

2.4. Tensile Strength Testing

The mechanical properties of the upcycled membranes were evaluated through tensile strength testing. Specimens were prepared by cutting the membranes into rectangular strips measuring 20 mm in length and 5 mm in width. Due to the inherent fragility of the upcycled Styrofoam matrix, which fell below the minimum force threshold of a universal testing machine, tensile strength was quantified using a high-precision manual pull-testing device. The peak force required to achieve specimen fracture was recorded. All measurements were conducted at room temperature (25 °C), and the reported values represent the average of five replicates to ensure statistical reliability.

2.5. Water Contact Angle (WCA) Analysis

Surface wettability, a critical determinant of water permeability and fouling resistance, was evaluated through water contact angle (WCA) measurements. To determine the static contact angle, a 5 µL droplet of deionized water was gently deposited onto the surface of the dried membrane using a precision micropipette. The resulting droplet profile was captured using a high-resolution digital microscope (Dino-Lite Edge 3.0 AM73915MZTL, AnMo Electronics, Taiwan). The contact angle was subsequently quantified using AutoCAD 2018 version software by measuring the angle at the solid–liquid interface. To ensure experimental reproducibility and accuracy, each membrane sample was tested in triplicate, and the results are reported as the mean values.

3. Results and Discussion

3.1. Membrane Morphology

Scanning electron microscopy (SEM) is an essential technique for elucidating the internal architecture and morphological transitions of polymeric membranes. Figure 2 presents the cross-sectional SEM micrographs of the raw Styrofoam and the various fabricated membranes. The raw Styrofoam, shown in Figure 2a, displays a characteristic network of interconnected hollow cells, reflecting its high air content. In contrast, the native Styrofoam membrane (Figure 2b) exhibits a distinct asymmetric structure consisting of a dense, spongy top layer and a supporting layer dominated by slender macrovoids. This structural differentiation is attributed to the temperature gradient and solvent/non-solvent exchange rate during the phase inversion process, which induces time-dependent nucleation phenomena [25].

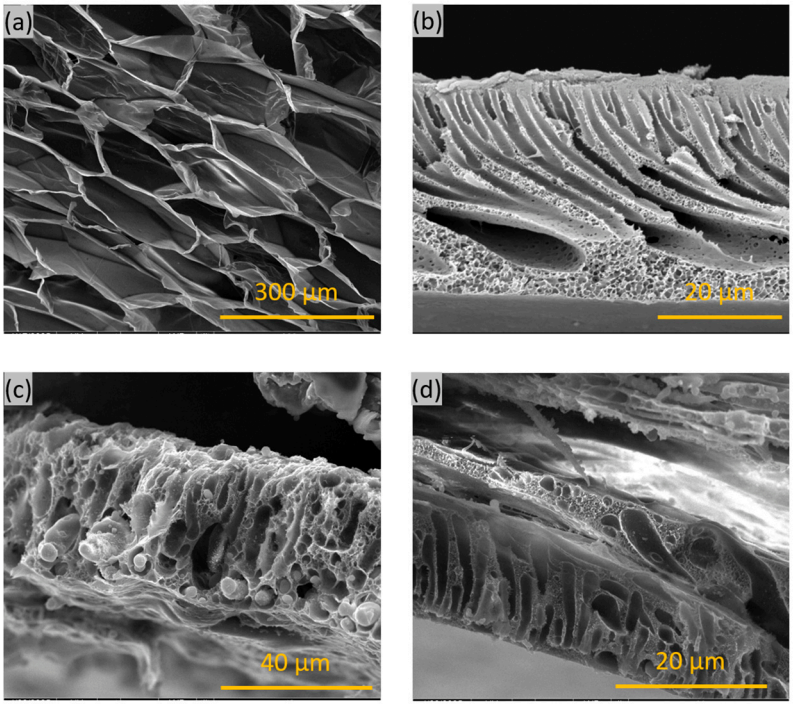


Figure 2. Cross-sectional SEM images: (**a**) Styrofoam food packaging (**b**) Native Styrofoam membrane (**c**) Styrofoam/PI membrane (**d**) Styrofoam/PI/TPU membrane.

Upon the incorporation of polyimide (PI) into the dope solution, Figure 2c illustrates the emergence of spherical inclusions within the macrovoids and pores. This additive facilitates a morphological transformation, where elongated, narrow macrovoids evolve into larger, more rounded void structures, consistent with previous work [21]. Furthermore, the addition of thermoplastic polyurethane (TPU) to the EPS/PI matrix introduced distinct layered domains in the central laminar region of the membrane (Figure 2d). These TPU-induced domains appear to interrupt the native finger-like macrovoid architecture, resulting in the formation of stacked laminar structures along the membrane's midsection.

Surface imaging is a standard approach for assessing the selective layer's morphology, ensuring structural integrity, and qualitatively evaluating surface roughness. Figure 3 presents the SEM micrographs of the top and bottom surfaces for the native Styrofoam and blended membranes. Following the incorporation of polyimide (PI), the top surface exhibits distinct circular features resembling craters (Figure 3). This morphological evolution is attributed to rapid solvent evaporation and the kinetics of liquid–liquid demixing during the phase inversion process [26]. Furthermore, the presence of multiple polymers

with disparate solidification rates influences the phase behaviour; the rapid precipitation of Styrofoam compared with PI upon non-solvent contact induces these localized structural variations.

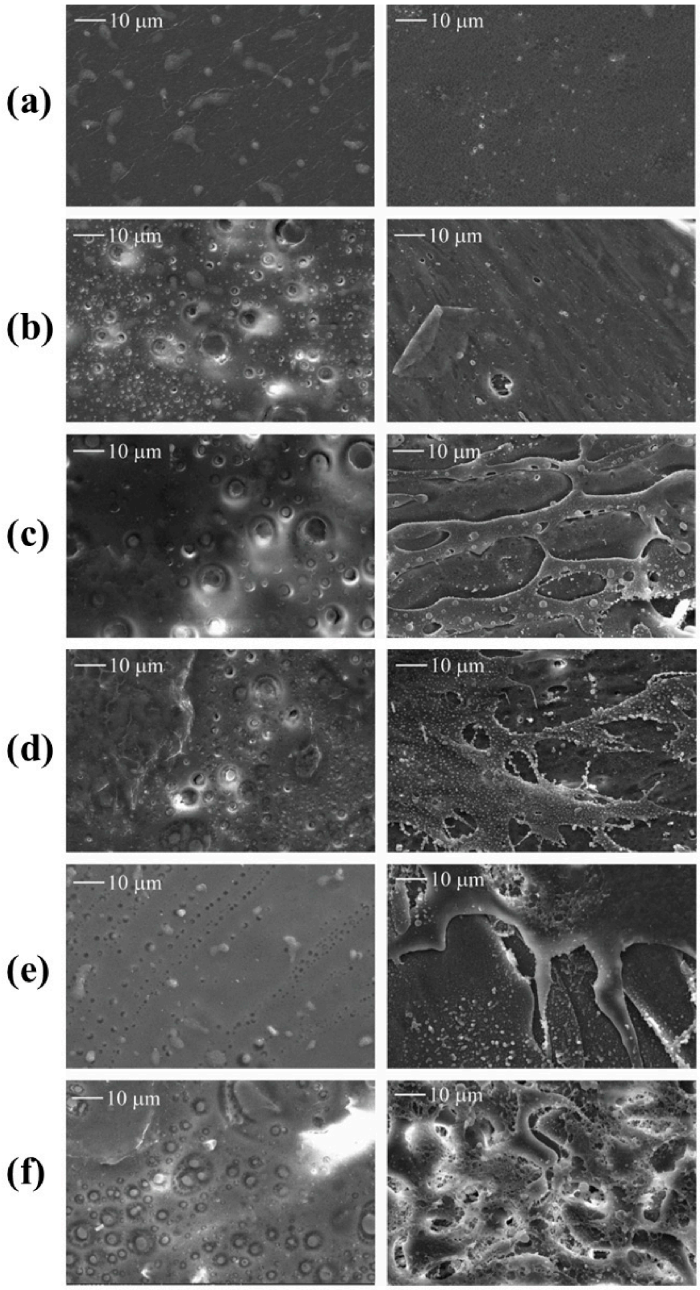


Figure 3. SEM micrographs showing the morphology of 20 wt. % Styrofoam blend membranes on top surfaces (**left**) and bottom surfaces (**right**): (**a**) #M0 (**b**) #M1 (**c**) #M2 (**d**) #M3 (**e**) #M4 (**f**) #M5.

On the bottom surfaces of the membranes (Figure 3c–f), solidified TPU domains are clearly visible, whereas the control samples (#M0 and #M1) remain free of such material. This localized deposition is likely governed by the differing thermal and phase inversion properties of the polymers. Since polystyrene precipitates more rapidly than TPU, the latter remains in the mobile phase longer, eventually solidifying on the bottom surface. The higher viscosity and slower solidification kinetics of TPU further inhibit its migration to the top selective layer. A similar morphological phenomenon has been documented in PTFE/TPU blends, where SEM analysis identified the development of fibril-like structures that scaled proportionally with additive concentration [27].

The cross-sectional morphology provides essential qualitative insights into how the varying polymer compositions dictate the final membrane architecture. Figure 4 illustrates the cross-sections of the upcycled blend membranes at multiple magnifications. In membranes synthesized via the wet phase inversion (NIPS) method, the structure typically bifurcates into two distinct regions: a dense, spongy top layer formed by rapid precipitation upon contact with the non-solvent, and a sub-layer characterized by elongated, finger-like macrovoids resulting from slower precipitation kinetics [28].

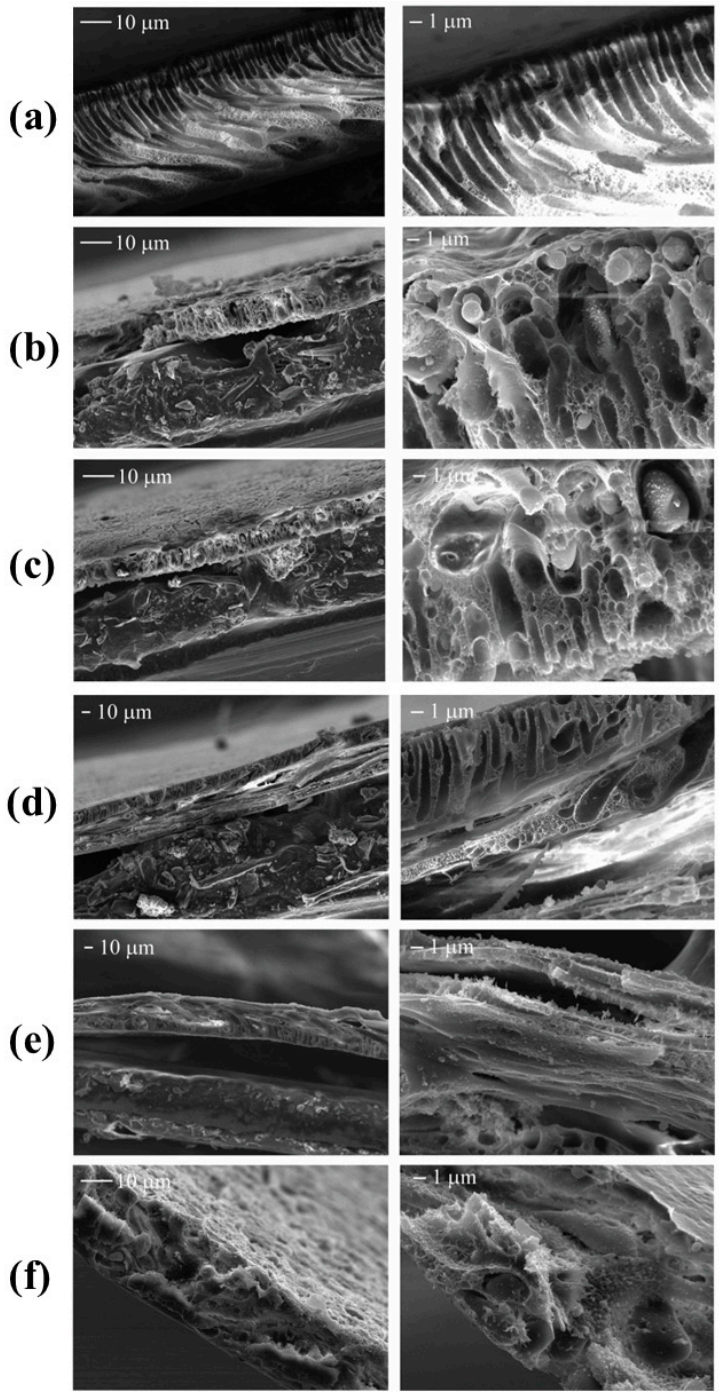


Figure 4. Cross-sectional SEM micrographs of 20 wt. % Styrofoam blended PI/TPU waste membranes with different magnification: (**a**) #M0 (**b**) #M1 (**c**) #M2 (**d**) #M3 (**e**) #M4 (**f**) #M5.

While previous work demonstrated that adding polyimide (PI) to a Styrofoam matrix induced the formation of mushroom-shaped structures within these macrovoids [21],

the introduction of TPU into the Styrofoam/PI system significantly altered this trajectory. Specifically, the emergence of stacked laminar formations effectively suppressed the vertical growth of the finger-like features. This structural evolution is likely driven by the disparate precipitation rates and thermodynamic affinities of the three polymer components. As the TPU concentration increased, the basal region of the membrane exhibited an increasingly rugged topography, eventually obscuring the original bottom surface (Figure 4c–f). This suggests that TPU acts as a structural modifier that disrupts the typical convective flow of solvent and non-solvent during the demixing process.

3.2. Mechanical Properties of Upcycled EPS/PI/TPU Membranes

To evaluate mechanical integrity, the membranes were air-dried and sectioned into rectangular specimens (20 mm × 5 cm × 100 μm). Due to the inherent brittleness of the upcycled Styrofoam matrix, the membranes exhibited negligible elongation prior to failure; thus, the recorded values represent the tensile strength at the point of fracture. Figure 5 illustrates the breaking tensile strength of the various upcycled formulations.

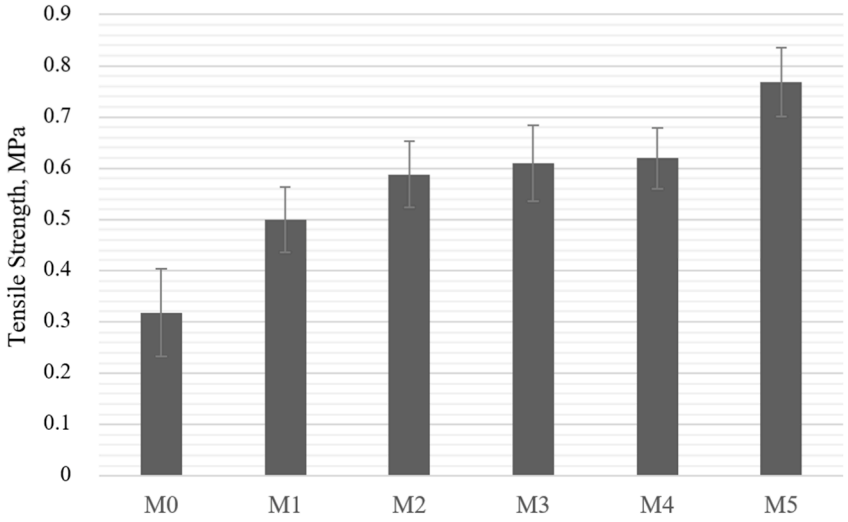


Figure 5. Tensile breaking strength of the upcycled membranes with increasing TPU concentration.

The native Styrofoam membrane was characterized by extreme fragility, with a recorded breaking strength of only 0.32 MPa. While our previous research efforts successfully enhanced rejection properties by incorporating polyimide (PI) [21] and polyvinylpyrrolidone (PVP) [29], those membranes remained too fragile for standardized tensile quantification. In this study, the introduction of thermoplastic polyurethane (TPU) waste recovered from 3D printing byproducts significantly bolstered the structural stability of the Styrofoam/PI matrix.

As shown in Figure 5, the breaking strength increased proportionally with TPU concentration, reaching a peak of 0.77 MPa, more than doubling the strength of the native membrane. TPU is well-regarded for its ability to tune the mechanical, thermal, and physical characteristics of polymer blends, particularly through its high tensile strength and controllable elasticity [30]. While commercial TPU flat-sheet membranes can achieve strengths up to 29.48 [31] and nanofiber variants reach 5.61 MPa [32], the primary objective here was the reclamation of waste materials.

The observed reinforcement is supported by SEM bottom-surface analysis (Figure 3c–f), which indicates that TPU precipitates primarily at the basal layer and within the midsection during phase inversion. This distribution acts as a structural scaffold, mitigating the inherent weaknesses of the polystyrene matrix. This phenomenon aligns with findings by

Wang et al. [33] and Mahdavi et al. [26], who demonstrated that the elastomeric properties of TPU can substantially reinforce traditionally brittle polymers such as PES.

3.3. Surface Wettability and Contact Angle Analysis

Water contact angle (WCA) analysis was employed as a primary metric to assess the surface hydrophilicity of the fabricated membranes, a factor that significantly influences both water permeability and fouling propensity. Figure 6 presents the WCA measurements for the various Styrofoam-based blend formulations.

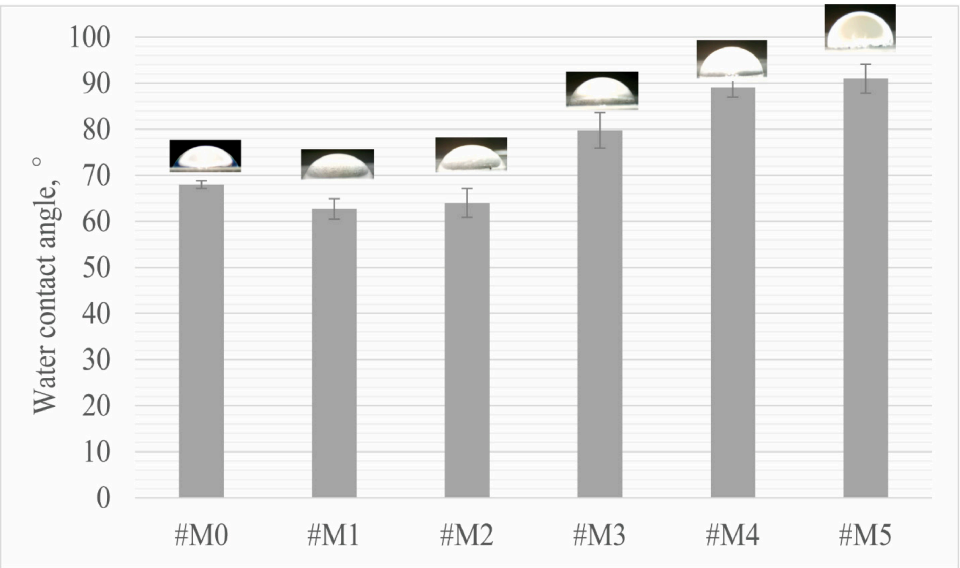


Figure 6. Water contact angle of Styrofoam/PI waste membranes with varied TPU concentration.

The pristine Styrofoam waste membrane (#M0) exhibited a WCA of 68°, aligning with values previously reported for waste-derived Styrofoam membranes [21]. Upon the incorporation of 6 wt.% polyimide (PI), the WCA initially decreased to 63°, suggesting a slight enhancement in surface wettability. While a similar composition in our previous research yielded a higher WCA of 84°, this variance is likely attributable to the inherent chemical inconsistencies found in post-consumer waste feedstock. Trace contaminants or varying degrees of degradation in the expanded polystyrene (EPS) can result in localized fluctuations in surface energy; however, both values remain firmly within the hydrophilic regime (WCA < 90°).

Conversely, the introduction of thermoplastic polyurethane (TPU) induced a progressive increase in hydrophobicity, with WCA values scaling proportionally with TPU concentration. This trend culminated in a WCA of 91° for sample #M5 (1 wt.% TPU), marking a transition into the semi-hydrophobic regime. This behavior is consistent with literature, where high-concentration TPU casting solutions (12 wt.%) have been shown to produce WCAs of approximately 83.3° [31].

This observed trend mirrors findings by Khaled et al. [34], who noted that membranes derived from high-impact polystyrene (HIPS) waste exhibit hydrophilic to semi-hydrophilic characteristics, unlike commercial polystyrene (PS) membranes, which are typically hydrophobic due to a lack of polar functional groups [35]. The discrepancy between commercial PS and waste-derived EPS/HIPS likely stems from the specific additives, flame retardants, and impurities present in post-consumer products. As evidenced by the surface morphology in Figure 3, these residual components and the added TPU effectively alter the membrane's surface topography and chemical composition, thereby driving the observed increase in hydrophobicity.

3.4. Filtration Performance: Rejection and Permeance Analysis

Membrane performance was evaluated through protein rejection and water permeance tests to determine the filtration characteristics of the upcycled formulations. Figure 7 illustrates the relationship between water flux and the rejection of two different molecular weight markers: Bovine Serum Albumin (BSA, 65 kDa) and Polyvinylpyrrolidone (PVP, 1300 kDa).

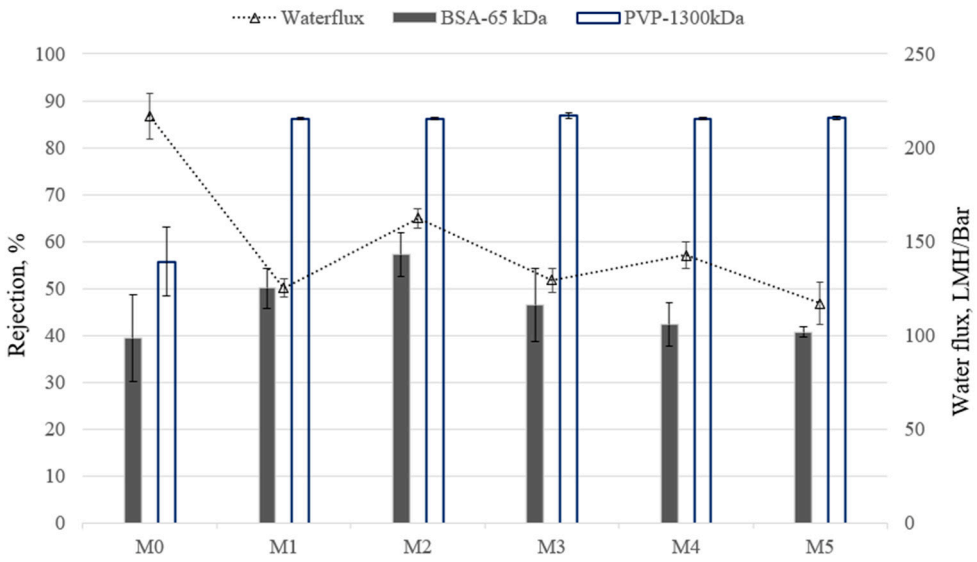


Figure 7. Protein rejection and water permeance of Styrofoam blend membranes with varied TPU concentration.

The native Styrofoam membrane (#M0) exhibited the highest water flux (214 LMH/bar) but the lowest rejection rates (39% for BSA and 55% for PVP), indicating a highly porous but non-selective structure with significant pore size distribution variability. The incorporation of 6 wt.% polyimide (PI) in formulation #M1 served as the optimized base for further modification, yielding a stabilized flux of 122 LMH/bar and improving BSA rejection to 50.9%. These results are consistent with our previous investigations into PS/PI blends [21].

The introduction of TPU waste induced a non-linear response in membrane performance. At a low concentration of 0.25 wt.% TPU (#M2), a synergistic effect was observed: water flux increased to 162.5 LMH/bar and BSA rejection peaked at 57.2%. This represented a 14% improvement in rejection over the #M1 base and a 44.9% increase over the native Styrofoam. This enhancement is likely due to moderate TPU-induced structural modifications where localized particle distributions facilitate the formation of preferential water channels without compromising selectivity [36].

However, as TPU concentrations increased beyond 0.25 wt.% (#M3–#M5), both BSA rejection and water permeance consistently declined, with rejection falling to 40.8% for sample #M5. The observed decline in membrane performance can be attributed to several interrelated factors, primarily rooted in the structural and chemical changes induced by higher TPU concentrations. As a non-porous additive, excessive TPU tends to cause physical pore blockage by obstructing surface openings and occupying the internal finger-like macrovoids, a phenomenon evidenced by the emergence of laminar layers in the SEM cross-sections. Furthermore, higher TPU loading can trigger particle agglomeration, which not only hinders separation efficiency but also restricts effective permeation pathways within the polymer matrix [37]. This physical resistance is compounded by a greater propensity for fouling; the increased hydrophobicity of TPU-rich domains, as confirmed by WCA analysis,

likely encourages the adsorption of BSA molecules within the finer pores, resulting in obstructive fouling that further diminishes water flux and rejection performance.

An interesting contrast was observed in the rejection of larger macromolecules. Regardless of the TPU concentration, all blended membranes (#M1–#M5) maintained a high and stable PVP rejection rate of approximately 86%. Compared with the globular, compact structure of BSA, the 1300 kDa PVP molecule is substantially larger and possesses a more flexible, extended configuration. This creates a bulkier hydrodynamic volume that is effectively excluded by the membrane matrix via size exclusion, even when finer pores are altered by TPU incorporation. These results confirm that while TPU modification influences ultrafiltration-range separation (BSA), the membranes remain highly effective for the removal of larger high-molecular-weight compounds.

4. Conclusions

This study demonstrates the successful upcycling of post-consumer Styrofoam packaging and 3D-printed thermoplastic polyurethane (TPU) waste into high-performance blend membranes using the non-solvent-induced phase separation (NIPS) technique. SEM characterization revealed that TPU incorporation fundamentally altered the internal membrane architecture, converting native finger-like macrovoids into reinforced laminar layers within the central core. Although the unmodified Styrofoam membrane yielded the highest water permeance, its selectivity was poor. The strategic addition of polyimide (PI) and TPU substantially enhanced overall separation efficiency. The formulation containing 0.25 wt.% TPU was identified as optimal, maximizing bovine serum albumin (BSA) rejection; higher TPU concentrations degraded performance due to agglomeration and pore blockage.

The blend membranes demonstrated a consistent rejection rate of ~86% for 1300 kDa macromolecules, confirming their viability for high-molecular-weight separations. Mechanically, TPU loading proportionally increased membrane robustness, achieving a peak tensile strength of 0.78 MPa—more than double that of the native matrix—while shifting the surface to a semi-hydrophobic state (91°). Ultimately, these findings prove that low concentrations of TPU waste can resolve the inherent fragility of Styrofoam membranes, providing a sustainable method for converting waste into functional filtration media.

While the dead-end filtration tests established intrinsic permeability, rejection, and mechanical viability, this setup does not perfectly mirror industrial conditions. Furthermore, while BSA rejection improved via pore contraction and altered wettability, the role of electrostatic interactions remains unquantified. Future research will evaluate the optimal 0.25 wt.% TPU membrane in a cross-flow module to assess long-term stability and cake layer mitigation. Additionally, in-depth electrokinetic studies—including pH-dependent zeta potential measurements—will be conducted to decouple the steric and electrostatic mechanisms driving separation.

Author Contributions: Conceptualization, T.S. and G.S.P.; methodology, T.T. and T.S.; validation, C.P.W., R.A.R., G.S.P. and N.M.; formal analysis, T.T., T.W. and G.S.P.; investigation, T.S.; resources, M.M. and N.M.; data curation, T.S. and T.W.; writing—original draft preparation, T.S. and R.A.R.; writing—review and editing, C.P.W. and G.S.P.; supervision, G.S.P.; project administration, C.P.W. and R.A.R.; funding acquisition, T.T., T.W., G.S.P., M.M., N.M., C.P.W. and R.A.R. All authors have read and agreed to the published version of the manuscript.

Funding: This research project received funding from Universitas Airlangga through the Hibah International Research Network program (Grant No. 3104/B/UN3.LPPM/PT.01.09/2024).

Institutional Review Board Statement: Not applicable.

Informed Consent Statement: Not applicable.

Data Availability Statement: The original contributions presented in this study are included in the article. Further inquiries can be directed to the corresponding author.

Conflicts of Interest: Tutik Sriani was employed by PT. Global Meditek Utama-IITOYA. All the authors declare that the research was conducted in the absence of any commercial or financial relationships that could be construed as a potential conflict of interest.

References

1. Dokl, M.; Copot, A.; Krajnc, D.; Fan, Y.F.; Vujanović, A.; Aviso, K.B.; Tan, R.R.; Kravanja, Z.; Čuček, L. Global projections of plastic use, end-of-life fate and potential changes in consumption, reduction, recycling and replacement with bioplastics to 2050. *Sustain. Prod. Consum.* **2024**, *51*, 498–518. [CrossRef]
2. Bianchi, M.S.; Cimadevila, M.; Trettnak, W. *Mare Plasticum—The Plastic Sea*, 1st ed.; Springer: Cham, Switzerland, 2020; pp. 250–252.
3. Kalali, E.N.; Lotfian, S.; Shabestari, M.E.; Khayatzadeh, S.; Zhao, C.; Nezhad, H.Y. A critical review of the current progress of plastic waste technology in structural materials. *Curr. Opin. Green Sustain. Chem.* **2023**, *40*, 100763. [CrossRef]
4. Gibb, B.C. Plastics are forever. *Nat. Chem.* **2019**, *11*, 394–395. [CrossRef] [PubMed]
5. Crespo, J.H.; Moreira, C.M.; Jervis, F.X.; Soto, M.; Amaya, J.L.; Banguera, L. Circular economy of expanded polystyrene container production: Environmental benefits of household waste recycling considering renewable energies. *Energy Rep.* **2022**, *8*, 306–311. [CrossRef]
6. Stoll, T.; Stoett, P.; Vince, J.; Hardesty, B.D. Governance and measures for the prevention of marine debris. In *Handbook of Microplastics in the Environment*; Rocha-Santos, T., Costa, M.F., Mouneyrac, C., Eds.; Springer: Cham, Switzerland, 2022; pp. 1129–1151.
7. Miraj, S.S.; Parveen, N.; Zedan, H.S. Plastic microbeads: Small yet mighty concerning. *Int. J. Environ. Health Res.* **2019**, *31*, 788–804. [CrossRef] [PubMed]
8. Jeon, S.; Jeon, J.H.; Jeong, J.; Kim, G.; Lee, S.; Kim, S.; Maruthupandy, M.; Lee, K.; Yang, S.I.; Cho, W.S. Size- and oxidative potential-dependent toxicity of environmentally relevant polystyrene Styrofoam microplastics to macrophages. *J. Hazard. Mater.* **2023**, *459*, 132295. [CrossRef] [PubMed]
9. Baghetto, V.; Sole, R.; Buranello, C.; Al-Abkal, M.; Facchin, M. Recent advancements in plastic packaging recycling: A mini-review. *Materials* **2021**, *14*, 4782. [CrossRef] [PubMed]
10. Xu, Z.; Sun, D.; Xu, J.; Yang, R.; Russell, J.D.; Liu, G. Progress and challenges in polystyrene recycling and upcycling. *ChemSusChem* **2024**, *17*, e202400474. [CrossRef] [PubMed]
11. Aguillar, A.M.G.; García, V.P.; Ávila, J.M.R. A thermo-catalytic pyrolysis of polystyrene waste review: A systematic, statistical, and bibliometric approach. *Polymers* **2023**, *15*, 1582. [CrossRef] [PubMed]
12. Gautam, B.; Huang, M.R.; Lin, C.C.; Chang, C.C.; Chen, J.T. A viable approach for polymer upcycling of polystyrene (Styrofoam) wastes to produce high-value predetermined organic compounds. *Polym. Degrad. Stab.* **2023**, *217*, 110528. [CrossRef]
13. Salvodelli, J.; Tomback, D.; Savoldelli, H. Breaking down polystyrene through the application of a two-step thermal degradation and bacterial method to produce usable byproducts. *Waste Manag.* **2017**, *60*, 123–126. [CrossRef] [PubMed]
14. Crespo, J.H.; Jervis, F.X.; Moreira, C.M.; Soto, M.; Amaya, J.L. Introduction of the circular economy to expanded polystyrene household waste: A case study from an Ecuadorian plastic manufacturer. *Procedia CIRP* **2020**, *90*, 49–54. [CrossRef]
15. Chen, D.; Xie, Z.; Ye, H.; Li, W.; Shi, W.; Liu, Y. Upcycling of expanded polystyrene waste: Amination as adsorbent to recover Eriochrome Black T and Congo red. *Sep. Purif. Technol.* **2022**, *289*, 120669. [CrossRef]
16. Pu, Y.; Xie, Z.; Ye, H.; Shi, W. Amidation modified waste polystyrene foam as an efficient recyclable adsorbent for organic dyes removal. *Water Sci. Technol.* **2021**, *83*, 2192–2205. [CrossRef] [PubMed]
17. Aprilita, N.H.; Ofens, T.F.P.; Nora, M.; Nassir, T.A.; Wahyuni, E.T. Conversion of styrofoam waste into a high-capacity and recoverable adsorbent for removing toxic Pb(II) from water media. *Glob. NEST J.* **2024**, *26*. [CrossRef]
18. Ye, H.; Xie, Z.; Li, W.; Pu, Y.; Liu, M.; Wen, Y.; Liu, Y. Converting waste polystyrene foam into value-added materials: A large-capacity scavenger to remove cationic dyes and heavy metals. *J. Appl. Polym. Sci.* **2022**, *139*, 51868. [CrossRef]
19. Baig, N.; Alghunaimi, F.I.; Saleh, T.A. Hydrophobic and oleophilic carbon nanofiber impregnated Styrofoam for oil and water separation: A green technology. *Chem. Eng. J.* **2019**, *360*, 1613–1622. [CrossRef]
20. Wang, C.; Wang, Q.; Yu, J.; Wang, X.; Wang, L.; Zhao, B.; Hao, L.; Liu, W.; Wang, Z.; Chen, H.; et al. Converting waste expanded polystyrene into higher-value-added hyper-crosslinked porous polymer for rapid and highly efficient adsorption of aflatoxins. *J. Clean. Prod.* **2023**, *408*, 137102. [CrossRef]
21. Sriani, T.; Mahardika, M.; Miki, N.; Wulandari, C.P.; Prihandana, G.S. Impact of polyimide on the recycling of waste expanded polystyrene foam into flat-sheet filtration membrane. *J. Mater. Cycles Waste Manag.* **2024**, *26*, 3745–3756. [CrossRef]

22. Ryu, S.; Oh, H.W.; Kim, J. A study on the mechanical properties and thermal conductivity enhancement through TPU/BN composites by hybrid surface treatment of boron nitride. *Mater. Chem. Phys.* **2019**, *223*, 607–612. [CrossRef]
23. Nanni, A.; Crosetta, L.; Fauci, G.L.; Biagi, F.; Parisi, M.; Colombo, D.; Colonna, M. Study of the mechanical properties of thermoplastic polyurethane (TPU) recycled from end-of-life ski-boots and techno-economic analysis of mechanical recycling processes. *Sustain. Chem. Pharm.* **2023**, *33*, 101059. [CrossRef]
24. Dong, M.; Li, Q.; Liu, H.; Liu, C.; Wujcik, E.K.; Shao, Q.; Ding, T.; Mai, X.; Shen, C.; Guo, Z. Thermoplastic polyurethane-carbon black nanocomposite coating: Fabrication and solid particle erosion resistance. *Polymer* **2018**, *158*, 381–390. [CrossRef]
25. Manickam, S.S.; McCutcheon, J.R. Understanding mass transfer through asymmetric membranes during forward osmosis: A historical perspective and critical review on measuring structural parameter with semi-empirical models and characterization approaches. *Desalination* **2017**, *421*, 110–126. [CrossRef]
26. Mahdavi, H.; Hosseini, F.; Heidari, A.A.; Karami, M. Polyethersulfone-TPU blend membrane coated with environmentally friendly sabja seed mucilage-Cu^{2+} cross-linked layer with outstanding separation performance and superior antifouling. *J. Ind. Eng. Chem.* **2023**, *121*, 421–433. [CrossRef]
27. Huang, A.; Peng, X.; Turng, L.S. In-situ fibrillated polytetrafluoroethylene in thermoplastic polyurethane via melt blending: Effect on rheological behavior, mechanical properties, and microcellular foamability. *Polymer* **2018**, *134*, 263–274. [CrossRef]
28. Mulder, M. *Basic Principles of Membrane Technology*, 2nd ed.; Kluwer Academic Publishers: Dordrecht, The Netherlands, 1996.
29. Sriani, T.; Mahardika, M.; Aldhama, S.A.; Wulandari, C.P.; Prihandana, G.S. Upcycling of expanded polystyrene waste-impregnated PVP using wet-phase inversion for effective microalgae harvesting. *Polymers* **2024**, *16*, 2703. [CrossRef] [PubMed]
30. Liu, L.C.; Liang, W.C.; Chen, C.M. Manufacture of recyclable thermoplastic polyurethane/silicone blends and their mechanical properties. *Manuf. Lett.* **2022**, *31*, 1–5. [CrossRef]
31. Sha, J.; Zuxin, C.; Zhu, L.; Xiao, K. Preparation of modified atmosphere and antifogging packaging membranes by blending modified polyvinyl alcohol with polyester-based thermoplastic polyurethane and its application in kiwifruits. *Food Packag. Shelf Life* **2024**, *43*, 101286. [CrossRef]
32. Zhang, C.; Li, J.; Chen, Y.; Zou, Z.; Zhang, Y.; Liu, Y.; Wu, B. Stretchable, flexible, and breathable MXene/dopamine/thermoplastic polyurethane nanofiber membrane with outstanding strain sensing and electromagnetic interference shielding performances. *Mater. Today Commun.* **2024**, *38*, 107968. [CrossRef]
33. Wang, W.; Ma, X.; Si, J.; Cui, Z.; Wang, Q.; Liu, X. Deacetylated cellulose acetate/polyurethane composite nanofiber membranes with highly efficient oil/water separation and excellent mechanical properties. *Macromol. Mater. Eng.* **2021**, *306*, 2100270. [CrossRef]
34. Khaled, M.; Noby, H.; Aissa, W.A.; El-Shazly, A.H. Facile fabrication of porous and hydrophilic polystyrene membranes using recycled waste. *Mater. Sci. Forum* **2020**, *1008*, 39–46. [CrossRef]
35. Li, J.; Yang, H.; Jiang, Q.; Jiang, B.; Jiang, L.; Xue, X.; Huang, W. Preparation and properties of ultra-high molecular weight polystyrene porous fiber membrane. *J. Porous Mater.* **2025**, *32*, 1683–1691. [CrossRef]
36. Essate, A.; Idrissi, D.E.M.I.; Achiou, B.; Adlane, S.; Breida, M.; Curcio, S.; Chakraborty, S.; Younssi, S.A.; Ouammou, M. High-performance zeolite-A/polystyrene composite membrane tailored for efficient soluble dyes separation and antifouling. *Colloids Surf. A Physicochem. Eng. Asp.* **2024**, *703*, 135162. [CrossRef]
37. Shi, W.; Gao, F.; Li, X.; Wang, Z. High zeolite loading mixed matrix membrane for effective removal of ammonia from surface water. *Water Res.* **2022**, *221*, 118849. [CrossRef] [PubMed]

Disclaimer/Publisher's Note: The statements, opinions and data contained in all publications are solely those of the individual author(s) and contributor(s) and not of MDPI and/or the editor(s). MDPI and/or the editor(s) disclaim responsibility for any injury to people or property resulting from any ideas, methods, instructions or products referred to in the content.